PROCEEDINGS OF SPIE

SPIEDigitalLibrary.org/conference-proceedings-of-spie

Large mode area double-clad ytterbium-doped tapered fiber with low birefringence

Andrei Fedotov, Vasilii Ustimchik, Joona Rissanen, Teppo Noronen, Regina Gumenyuk, et al.

Andrei Fedotov, Vasilii Ustimchik, Joona Rissanen, Teppo Noronen, Regina Gumenyuk, Yuri Chamorovskii, Alexander Kolosovskii, Victor Voloshin, Igor Vorob'ev, Valery Filippov, "Large mode area double-clad ytterbium-doped tapered fiber with low birefringence," Proc. SPIE 11665, Fiber Lasers XVIII: Technology and Systems, 116651T (5 March 2021); doi: 10.1117/12.2577834

SPIE.

Event: SPIE LASE, 2021, Online Only

Large mode area double-clad ytterbium-doped tapered fiber with low birefringence

Andrei Fedotov*[a], Vasilii Ustimchik[b], Joona Rissanen[c], Teppo Noronen[c], Regina Gumenyuk[a], Yuri Chamorovskii[d], Alexander Kolosovskii[d], Victor Voloshin[d], Igor Vorob'ev[d], Valery Filippov[c]
[a]Tampere University, Kalevantie, 33100 Tampere, Finland; [b]Peter the Great St. Petersburg Polytechnic University, Polytechnicheskaya str. 29, 195251 St.Petersburg, Russian Federation; [c]Ampliconyx Ltd, Lautakatonkatu 18, 33580 Tampere, Finland, [d]Kotel'nikov Institute of Radio Engineering and Electronics (Fryazino Branch) Russian Academy of Science, Vvedenskogo Sq.1, 141190 Fryazino, Russian Federation

ABSTRACT

We developed ytterbium-doped double-clad large mode area (MFD = 30 μm) spun tapered fibers with low internal birefringence and perfect beam quality (M^2 < 1.2). Picosecond MOPA system (95ps/100 MHz, 1064 nm) based on proposed active tapered fiber with output average power of 64 W (gain 32 dB) is demonstrated.

Keywords: polarization, birefringence, fiber laser, active spun fiber, active tapered fiber, ultrafast fiber amplifier

1. INTRODUCTION

The technology of high-power pulsed fiber amplifiers requires large mode area (LMA) polarization maintaining (PM) active fibers. Currently, three main types of fibers are used for these purposes: LMA PM fibers with low numerical aperture (NA) [1], micro-structured active fibers [2], and PM tapered double clad fibers (T-DCF) [3]. Polarization maintaining in all these types of fibers is achieved by inducing strong internal stresses (PANDA or stressed clad technology). High temperature sensitivity of birefringence at active fibers with strong internal stresses is a significant disadvantage of these type of fibers [4-7]. It is especially important for active fibers, since they are always subject to inevitable internal heating caused mostly by a quantum defect [8]. As a rule, strong pumping of active PM fiber leads to a rather rapid deterioration of the polarization extinction ratio (PER) [9].

The temperature sensitivity of birefringence is proportional to the value of the induced internal birefringence itself [4-7]. In order to solve the problem of the state of polarization (SOP) drift due to heating of PM active fiber clad under intense pumping, we recently have proposed using active fibers with low intrinsic birefringence (active SPUN fibers) [10, 11]. In [10, 11], an Yb-doped double clad tapered spun fiber (sT-DCF) with a 26 μm (core 35 μm) mode field diameter (MFD) was demonstrated. The first manufactured sT-DCF in [10, 11] had certain drawbacks:

- the MFD was limited by 26 μm (35 μm core);
- the spinning pitch varied along the length of the sT-DCF from 6 mm (at wide side) to 13 mm (at narrow side) due to imperfect drawing technology;
- the polarization eigenstates and the value of intrinsic birefringence were not measured.

Within the framework of presented paper, we have fabricated an active sT-DCF with MFD as large as 30 μm (core diameter was 44 μm). For this, we have developed an original technology for drawing of an active sT-DCF with constant pitch along the entire length. sT-DCF with 7.5, 15 and 30 mm pitches were manufactured. Polarization eigenstates and birefringence were measured for manufactured sT-DCFs. The 95 picosecond MOPA with an output power of 64 W and stable output SOP comprising sT-DCF is demonstrated.

Fiber Lasers XVIII: Technology and Systems, edited by Michalis N. Zervas, Cesar Jauregui-Misas, Proc. of SPIE Vol. 11665, 116651T · © 2021 SPIE
CCC code: 0277-786X/21/$21, doi: 10.1117/12.2577834

2. EXPERIMENT

2.1 Manufacturing of sT-DCF with constant pitch

An ytterbium-doped preform with step-index core was assembled with a 1:11 CCDR (Fig. 1a). The in-core absorption was 550 dB/m at 976 nm. The core numerical aperture was 0.1. To improve clad pump absorption in sT-DCF, the first cladding was four times truncated into a square shape with rounded corners as it shown Fig. 1a.

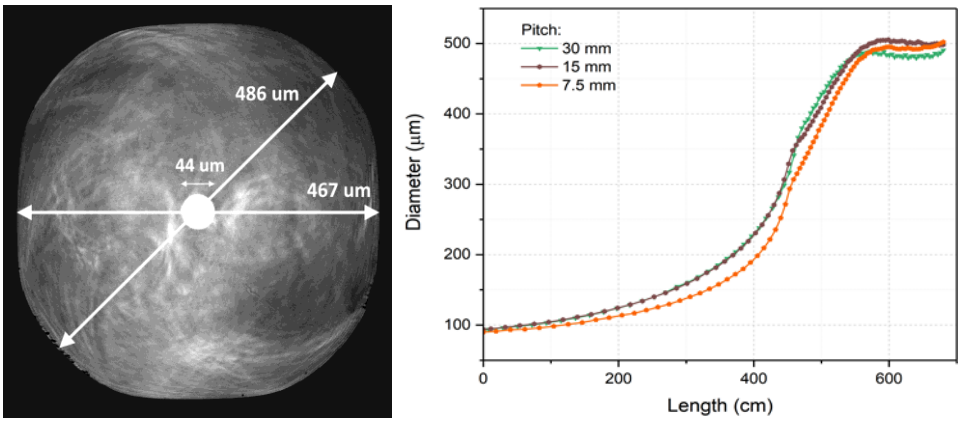

a) b)

Figure 1. a) End face view at the wide side of sT-DCF. b) Clad diameter of sT-DCF vs length.

sT-DCF was manufactured using a similar technology that was previously used for a passive [12-14] and active spun fibers [10, 11]. During drawing process, the preform was fed into the high-temperature furnace with a certain speed. The only difference from [10, 11] is that now the angular velocity of rotation has been synchronized with the drawing speed of the T-DCF. The key element of drawing tower for making of sT-DCF was the high precision spinning mechanism with the very wide range of rotation speed and precise alignment of a preform to avoid eccentricity preform relative to the drawing axis. To obtain fiber tapering, we changed all of the above-mentioned parameters (speed of preform feed, angular velocity of preform rotation and speed of drawing) in accordance with a predetermined algorithm. This is a way to obtain a given constant rotation pitch along the length of the sT-DCF.

Thus, the core/cladding diameter varied from 44/486 µm dawn to 8/90 µm along the length of 6.7 m. The longitudinal profiles of each of sT-DCF are shown in Fig. 1b. We have manufactured three different types of sT-DCF with same lengths and longitudinal shapes but with different pitch lengths: 7.5 mm, 15 mm and 30 mm (Fig. 1b.). The sT-DCFs were coated by low index primary reflecting coating (NA ≈ 0.4) and secondary protecting acrylate coating.

2.2 Beam properties and internal birefringence measurements

For all manufactured sT-DCFs with different pitches, we have measured the MFD, beam quality, type of birefringence, and its absolute values. Figure 2 shows the results of the near field distribution and M^2 measurements for the sT-DCF with different pitch values (7.5, 15 and 30 mm).

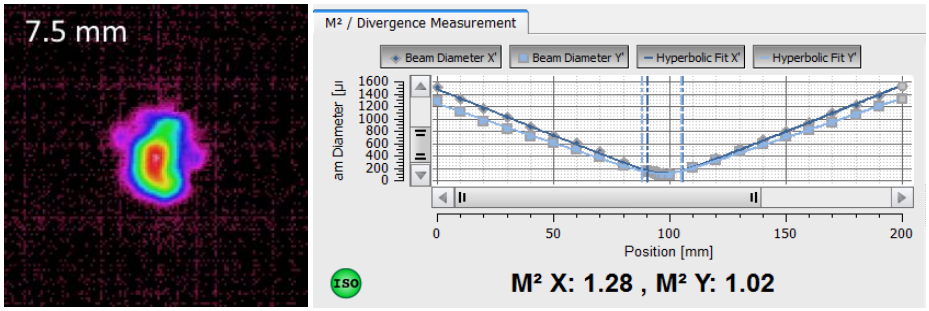

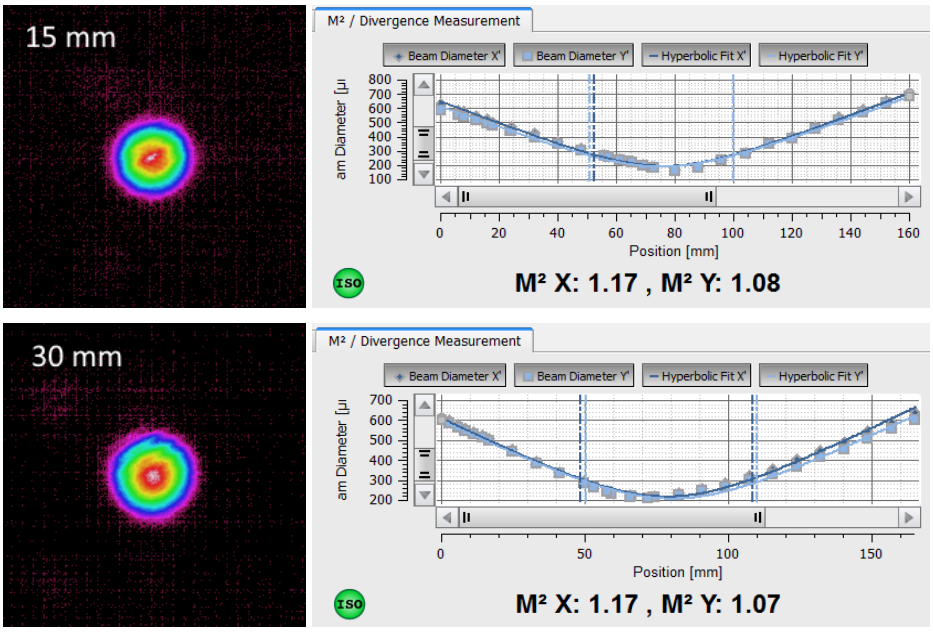

Figure 2. Shape of the beam and M^2 measurements results for sT-DCF with different pitches.

The main parameters of the measured beams are listed in Table 1.

Table 1. Beam properties for sT-DCF with different pitches

Pitch length, mm	Core diameter, μm	Beam shape	Spatial polarization distribution	MFD, μm	M^2_x / M^2_y
7.5	44	Non-regular	Uniform	30×22	1.28/1.02
15	44	Round	Uniform	30	1.17/1.08
30	44	Round	Uniform	31	1.17/1.07

The polarization eigenstates of sT-DCF were measured using Jones method [15]. The transfer Jones matrix of an optical device can be found by measuring output polarization states in response to known launched polarization states, similarly to how it was done in [16]. We have measured eigenstates using the technique proposed in [16]. The birefringence was calculated by knowing the linear one associated with bending (75 cm) and the ratio of linear and circular birefringence obtained from the Jones matrix.

In our measurements, a sT-DCF was positioned to have a large bend radius (75 cm) to reduce linear birefringence caused by macro bending during experimental studies. However, unavoidable bending and residual internal twist stresses always exist and therefore induce both linear and circular birefringence in any fibers. The eigenstates of sT-DCF are elliptical and close to circular (Fig. 3).

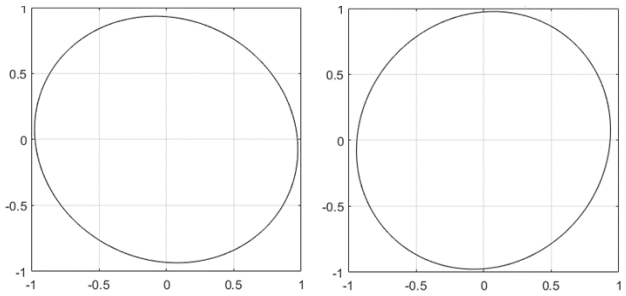

Figure 3. Shape of polarization eigenstates for sT-DCF with L_{pitch} = 15 mm.

The results of measuring eigenstates and internal birefringence for spun tapered fibers with different pitches are shown in Table 2.

Table 2. Measured eigenstates and birefringence for sT-DCFs

Pitch, mm	Ellipticity of eigenstates, degree	Azimuth of eigenstates, degree	Circular birefringence	Linear birefringence
7.5	-41.0/40.5	37.7/-53.9	4.12×10^{-8}	6.16×10^{-9}
15	42.3/-42.5	-30.5/57.6	7.59×10^{-8}	6.83×10^{-9}
30	-39.2/39.6	14.0/-77.1	3.36×10^{-8}	6.67×10^{-9}

2.3 Picosecond MOPA system with sT-DCF

To compare amplification properties of three spun tapered double-clad fibers we built a MOPA system shown in Figure 4. A commercially available gain-switched laser diode delivered 95 ps pulses was used as a seed laser. The repetition rate was 100 MHz. A linearly polarized signal with the linewidth of 20 pm was pre-amplified up to 40 mW and launched to the narrow end of the sT-DCF through the high-power isolator. sT-DCF was pumped by 976 nm laser diode only from the wide end in a free space using. The pump light was injected via the dichroic mirror and focusing lens. We only cooled the first 15 cm of the wide end to prevent any damage to the polymer coating due to intense pumping. The rest of tapered fibers was coiled on a metal plate and was not specially cooled. We deliberately tested the spun tapered fibers under harsh conditions in order to reveal the temperature dependence of the polarization state most clearly.

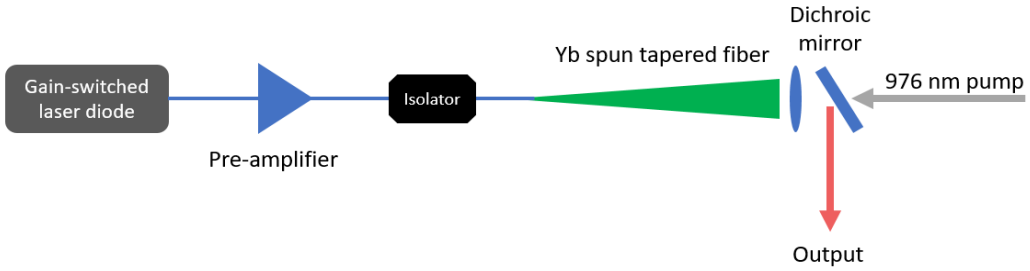

Figure 4. Experimental setup scheme

Among the investigated sT-DCFs the highest stability of the polarization state was demonstrated by a spun tapered fiber with 15 mm pitch. Therefore, amplification results presented for this particular sT-DCF. When pumped 100 W, the maximum output power was 64 W which corresponds to 32 dB gain (Fig. 5a). The spectrum was free of nonlinear effects and demonstrated ASE-to-signal contrast of 30 dB (Fig. 5b).

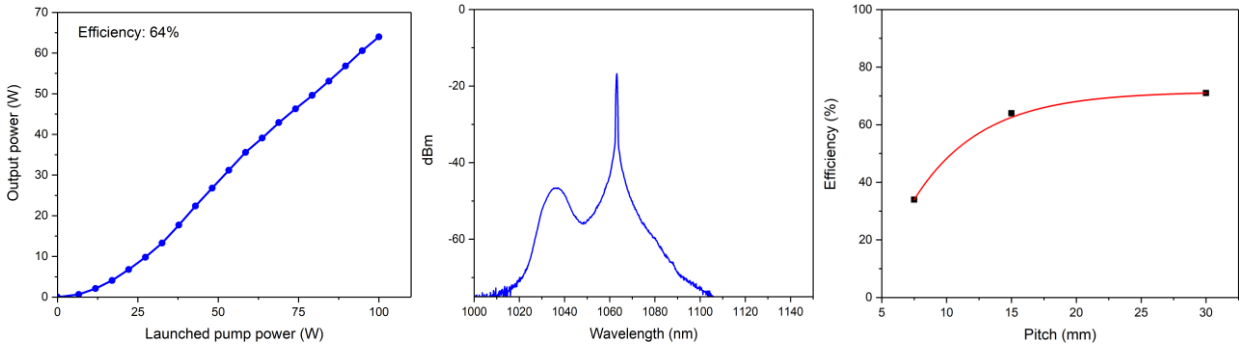

Figure 5. a) Dependence of output power on pump power and b) spectrum of the output signal for sT-DCF with 15 mm pitch; c) efficiency vs sT-DCF pitch.

Degree of polarization of the output decreased from 99% to 95% at maximum pump power of 100 W. The azimuth of polarization state of the output remained constant (Fig. 6a), while ellipticity deteriorated from 0 to 6.7 degree.

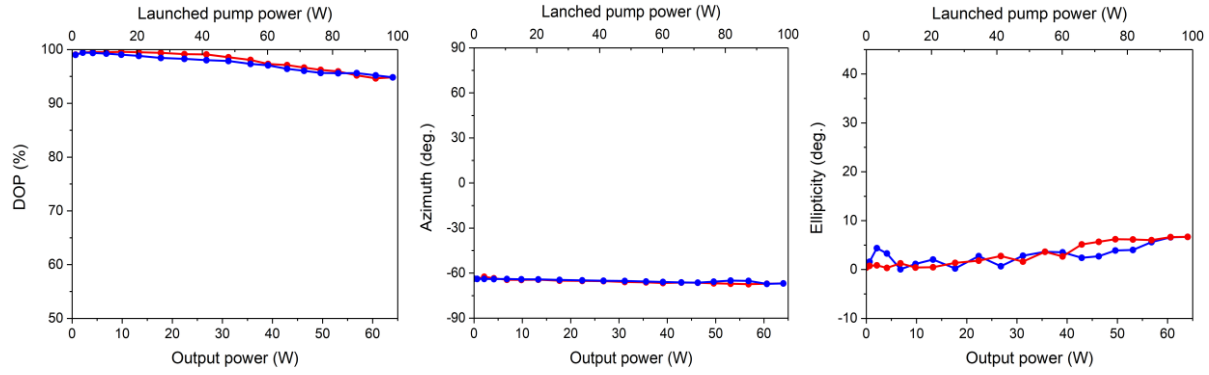

a) b) c)

Figure 6. a) Degree of polarization of output radiation as function of launched pump power/output power for sT-DCF with 15 mm picth. State of polarization versus launched pump power: (a) azimuth vs launched/output power and (b) ellipticity vs launched/output power.

3. DISCUSSION

Doping silica with Al or P causes significant mechanical stresses in the core of preforms (and then fibers) [17-19], which leads to appearance of strong local birefringence. Doping with rare-earth ions and drawing of an active optical fiber is accompanied by the formation even stronger local mechanical stresses in the core, which are inhomogeneous both in cross-section [17-20] and along the fiber length [21,22]. It was demonstrated in [17] that doping by Yb^{3+} ions leads to significant mechanical stresses and local changes in the refractive index up to 10^{-4}. Thus, the optical properties of an active optical fiber are substantially longitudinally inhomogeneous. Light depolarization caused by the doping-induced internal stresses, is the main obstacle for the development of an active fiber suitable for the efficient amplification of polarized light.

The goal of this work is to create a large MFD active fiber preserving a stable DOP. The idea of twisting an active fiber by hundreds times is simple: polarized light propagating in a fiber will spend on average the same time in the “fast” and “slow” axis of each local birefringence perturbation and, as a result, this fiber becomes close to an *uniform perfect fiber without any birefringence (or very small birefringence)* with polarization modes are degenerate by the propagation constant.

Three types of active sT-DCFs with the same length of 670 cm and differed pitch lengths (7.5, 15 and 30 mm) constant along the length were manufactured from the same preform. Therefore, different kinds sT-DCF correspond to the number of revolutions 870, 430 and 220.

We experimentally demonstrated that spinning of a preform during drawing minimizes the effect of the local mechanical stresses causing light depolarization and makes it possible to obtain sT-DCF with a small intrinsic birefringence (10^{-8}), which practically does not depolarize amplified radiation (Fig. 6a, DOP 95%).

Thus, we have demonstrated that when using a T-DCF, it is possible to build an amplifier with 95% DOP of output radiation, 30 μm MFD ($M^2 < 1.2$), 64% slope efficiency with very low near circular eigen birefringence. Basically, we expected the better amplifier performance (better DOP and smaller birefringence) for lower pitch (bigger number of revolutions). However, the situation is not so straightforward. At low pitches (7.5 mm) and 500 μm fiber clad diameter, elastic torsional mechanical stresses are “frozen” into the fiber clad, as it can be clearly seen in Fig. 7.

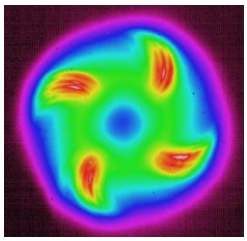

Figure 7. Clad pumped sT-DCF with 7.5mm pitch: far field image of end face.

Due to the photo-elastic effect, torsional stresses lead to the refractive index modulation in the cross section of the sT-DCF, which, in turn, causes the distortion of the output beam shape and, accordingly, to M^2 deterioration (Fig. 2, 7.5 mm pitch). Excessive twisting stresses appear to create periodic longitudinal modulation of the refractive index, making spun fiber similar to a Lyot depolarizer [23]. It leads to deterioration in DOP for fibers with 7.5mm pitch (Fig. 4) compared to fibers with longer pitches (15 mm and 30 mm).

The sT-DCF clad has a fancy shape. First, the sT-DCF clad is four times truncated to improve clad pump absorption (Fig. 1). In addition, the sT-DCF is twisted along the axis with a period of several millimeters and the outer diameter changes along the fiber axis. Certainly, all these measures ultimately lead improving of clad absorption but simultaneously, some part of unabsorbed pump power will be lost of due to vignetting. This leads to a visible deterioration of amplifier efficiency with pitch decreasing (Fig. 5c). The sT-DCF with a large pitch (30 mm) has better conversion efficiency, but DOP suffers, since the number of rotations is not enough to average all internal inhomogeneties.

We can conclude that there is a certain optimum for the length of the pitch, which allows delivering sT-DCF with optimal parameters (DOP, MFD and slope efficiency). The optimal pitch length is determined by the pump absorption, desirable MFD and the wide side clad diameter of sT-DCF. In our case, when the cladding has a diameter of 480 μm and the absorption is 550 dB/m, the optimal pitch is 15 mm, which allows us to create an amplifier with the abovementioned parameters. sT-DCF parameters optimization will be the subject of our further research.

4. CONCLUSION

We have implemented and conducted comparative studies of three types of ytterbium-doped spun tapered double clad fibers with different pitches (7.5, 15 and 30 mm) in this work. sT-DCF was used as an amplifier with 95% DOP of output radiation, 30 μm MFD (M^2 < 1.2), 64% slope efficiency and low near circular birefringence (~10^{-8}) is demonstrated. Picosecond MOPA system (95ps/100 MHz, 1062 nm) with proposed active fiber and output average power of 64 W (gain 32 dB) is presented.

ACKNOWLEDGEMENTS

This work was supported by the Academy of Finland Flagship Programme, Photonics Research and Innovation (PREIN), decision 320165, and a grant from the Russian Science Foundation (project No. 19–79-00371). Some of the investigated tapered fibers were developed at FIRE RAS in the framework of the State Task.

REFERENCES

[1] D. A. V. Kliner, J. P. Koplow, L. Goldberg, A. L. G. Carter, and J. A. Digweed, “Polarization-maintaining amplifier employing double-clad bow-tie fiber,” Opt. Lett. **26**, 184–186 (2001).

[2] O. Schmidt, J. Rothhardt, T. Eidam, F. Röser, J. Limpert, A. Tünnermann, K. Hansen, C. Jakobsen, and J. Broeng, “Single-polarization large-mode-area Yb-doped photonic crystal fiber,” in *Conference on Lasers and ElectroOptics/Quantum Electronics and Laser Science Conference and Photonic Applications Systems Technologies*, (Optical Society of America, 2008), p. CMB2.

[3] A. Fedotov, T. Noronen, R. Gumenyuk, V. Ustimchik, Y. Chamorovskii, K. Golant, M. Odnoblyudov, J. Rissanen, T. Niemi, and V. Filippov, “Ultra-large core birefringent Yb-doped tapered double clad fiber for high power amplifiers,” Opt. Express **26**, 6581–6592 (2018).

[4] A. Ourmazd, M. P. Varnham, R. D. Birch, and D. N. Payne, “Thermal properties of highly birefringent optical fibers and preforms,” Appl. Opt. **22**, 2374–2379 (1983).
[5] S. C. Rashleigh and M. J. Marrone, “Temperature dependence of stress birefringence in an elliptically clad fiber,” Opt. Lett. **8**, 127–129 (1983).
[6] S. Rashleigh, “Origins and control of polarization effects in single-mode fibers,” J. Light. Technol. **1**, 312–331 (1983).
[7] I. Kaminow, “Polarization in optical fibers,” IEEE J. Quantum Electron. **17**, 15–22 (1981).
[8] D. C. Brown and H. J. Hoffman, “Thermal, stress, and thermo-optic effects in high average power double-clad silica fiber lasers,” IEEE J. Quantum Electron. **37**, 207–217 (2001).
[9] F. Wellmann, M. Steinke, F. Meylahn, N. Bode, B. Willke, L. Overmeyer, P. Weßels, J. Neumann, and D. Kracht, “Low-noise, single-frequency 200 W fiber amplifier,” in *Fiber Lasers XVII: Technology and Systems*, vol. 11260 L. Dong, ed., International Society for Optics and Photonics (SPIE, 2020), pp. 125 – 131.
[10] J. Rissanen, A. Fedotov, T. Noronen, R. Gumenyuk, Yu. Chamorovskiy, A. Kolosovskii, V. Voloshin, I. Vorobev, M. Odnoblyudov and V. Filippov "Large-mode-area double clad ytterbium-doped tapered fiber with circular birefringence", Proc. SPIE 10897, Fiber Lasers XVI: Technology and Systems, 1089725 (7 March 2019).
[11] 11. A. Fedotov, V. Ustimchik, Y. Chamorovskii, R. Gumenyuk and V. Filippov, "Low-birefringence Active Tapered Fibers for High-power Applications," in *OSA Advanced Photonics Congress (AP) 2020 (IPR, NP, NOMA, Networks, PVLED, PSC, SPPCom, SOF)*, L. Caspani, A. Tauke-Pedretti, F. Leo, and B. Yang, eds., OSA Technical Digest (Optical Society of America, 2020), paper SoTu2H.7.
[12] Y. Chamorovskiy, N. Starostin, M. Ryabko, A. Sazonov, S. Morshnev, V. Gubin, I. Vorob’ev, and S. Nikitov, “Miniature microstructured fiber coil with high magneto-optical sensitivity,” Opt. Commun. **282**, 4618 – 4621 (2009).
[13] A. J. Barlow, J. J. Ramskov-Hansen, and D. N. Payne, “Birefringence and polarization mode-dispersion in spun single-mode fibers,” Appl. Opt. **20**, 2962–2968 (1981).
[14] D. N. Payne, A. J. Barlow, and J. J. Ramskov Hansen, “Development of low- and high-birefringence optical fibers,” IEEE Transactions on Microw. Theory Tech. **30**, 323–334 (1982).
[15] 15. R. C. Jones, “A new calculus for the treatment of optical systems. VI. experimental determination of the matrix∗,” J. Opt. Soc. Am. **37**, 110–112 (1947).
[16] Y. Wang, C.-Q. Xu, and V. Izraelian, “Characterization of spun fibers with millimeter spin periods,” Opt. Express **13**, 3841–3851 (2005).
[17] S. Unger, J. Kirchhof, V. Reichel, and H. Bartelt, “Ytterbium-doping related stresses in preforms for high-power fiber lasers,” J. Light. Technol. **27**, 2111–2116 (2009).
[18] G. W. Scherer, “Stress-induced index profile distortion in optical waveguides,” Appl. Opt. **19**, 2000–2006 (1980).
[19] O. E. Shushpanov, A. N. Tuzov, I. V. Alexsandrov, S. P. Vikulov, M. E. Zhabotinskii, V. V. Romanovtzev, and S. J. Feld, “An automated system for measurement of mechanical stresses in optical fiber preforms with polarization-optical method,” Radiotechnika pp. 67–72 (1988).
[20] M. R. Hutsel, R. Ingle, and T. K. Gaylord, “Accurate cross-sectional stress profiling of optical fibers,” Appl. Opt. **48**, 4985–4995 (2009).
[21] Z. Lou, B. Yang, K. Han, X. Wang, H. Zhang, X. Xi, and Z. Liu, “Real-time in-situ distributed fiber core temperature measurement in hundred-watt fiber laser oscillator pumped by 915/976 nm LD sources,” Sci. Reports **10**, 9006 (2020).
[22] F. Just, R. Spittel, J. Bierlich, S. Grimm, M. Jäger, and H. Bartelt, “The influence of the fiber drawing process on intrinsic stress and the resulting birefringence optimization of pm fibers,” Opt. Mater. **42**, 345 – 350 (2015).
[23] W. Burns, “Degree of polarization in the lyot depolarizer,” J. Light. Technol. **1**, 475–479 (1983).